Room-temperature photon avalanche up-conversion in Er-doped fluoride glass and fibre pumped at 700 nm

1995 J. Phys.: Condens. Matter 7 3363

(http://iopscience.iop.org/0953-8984/7/17/018)

J. Phys.: Condens. Matter 7 (1995) 3363–3370. Printed in the UK

Room-temperature photon avalanche up-conversion in Er-doped fluoride glass and fibre pumped at 700 nm

Yihong Chen†, Daniel Meichenin‡ and Francois Auzel‡

† Shanghai Institute of Optics and Fine Mechanics, Chinese Academy of Sciences, PO Box 800-216, Shanghai, People's Republic of China

‡ France Telecom, Centre National d'Etudes des Télécommunications, Paris B, Laboratoire de Bagneux, BP 107, 92225 Bagneux Cédex, France

Received 19 July 1994, in final form 7 December 1994

Abstract. A strong emission at 550 nm as well as a series of other wavelengths have been observed in Er-doped ZrF_4–BaF_2–LaF_3–AlF_3–NaF fibres and bulk glass at room temperature when the excitation wavelength is about 700 nm, which is far away from the absorptions from the ground state of Er^{3+} ions. Measurements of excitation, time delay and intensity dependence versus pump power suggest that these emissions are caused by the photon avalanche effect originating from the multiphonon side-band absorption. The excitation mechanisms of this photon avalanche have been analysed. Spectral measurement also show some strong emissions in the IR region, some features of which are probably linked with laser action.

The up-conversion emission phenomenon of ions when excitation is far away from ground-state absorptions to electronic levels has been found in several rare-earth- and transition-metal-ion-doped halide and oxide crystals. This phenomenon is known as the 'photon avalanche' which refers to the change in the order of magnitude of the fluorescence when the pump intensity varies from below to above a certain critical threshold. This non-linear effect is related to the cumulative absorption from an excited state. The first system which demonstrated this property was a Pr^{3+}:$LaCl_3$ crystal [1, 2]. Then similar phenomena were observed in the Sm^{3+}:$LaBr_3$ [3], Nd^{3+}:$YLiF_4$ [4], Ni^{2+}:$CsCdCl_3$ [5], Nd^{3+}:$La_xCe_{1-x}Cl_3$ [6] and Tm:$YAlO_3$ [7] systems. All these operations were in crystals and most were at low temperatures. In recent work [8], we demonstrated that this effect could also exist in a ZrF_4–BaF_2–LaF_3–AlF_3–NaF (ZBLAN) glass doped with Er^{3+} ions at room temperature. When excited at 579.2 nm, an extremely long rise time of several seconds was found; the threshold for the photon avalanche was as high as 60 kW cm^{-2}. Soon after that, we considered an erbium-doped ZBLAN fibre, in which a strong avalanche green emission was observed at room temperature with an incident power threshold as low as 5 mW [9]. This could make this material of practical interest for an avalanche-pumped laser [10]. Quite recently, some features of the avalanche effect were observed in a Pr-doped silica fibre [11]. In this paper we report the properties of another photon avalanche that we have achieved in Er: ZBLAN glass and fibre when excited at about 700 nm. The avalanche in this pump scheme is found to be even more efficient than that pumped at 579 nm, and some strong emissions in the IR region have also been observed for the fibre.

Single-mode ZBLAN fibres doped with 3% ErF_3 and bulk ZBLAN glass with the same concentration have been used in this research. Two pieces of the fibre with lengths of 8 and 90 cm have been studied. The fibre ends had been polished. Pumping was provided

0953-8984/95/173363+08$19.50

by an argon-laser pumped Ti:sapphire laser operating between 690 and 1000 nm or a DCM dye laser operating between 620 and 710 nm. The pump light was focused by a 25× objective into either the fibre or the bulk sample; the dimension of the beam waist is about 6 μm. The spectra were measured using a Jobin–Yvon double-grating monochromator with an EMI9658B(S-20) photomultiplier and a Ge detector for the infrared part of the spectra. Rise times were measured with a Tektronix 2230 oscilloscope.

The avalanche threshold effect was observed for both samples when pumped at 690 nm; for the bulk sample, the threshold incident power is about 100 mW for the appearance of the up-converted green emission, but for the fibre, it is about 4 mW. The threshold value changes with the pump wavelength. As soon as the pump power reaches the threshold, a uniform pattern of separated dots of green emission can be clearly observed along the fibre; the separation distance between two neighbouring dots is about 1 mm; every one of these dots consists of about six even smaller dots when examined with a microscope (figure 1). Besides these, structures with a longer period of about 1–10 cm can also be observed sometimes. On increase in pump power, the dots expanded and finally connected with each other; such dots are not observed in the bulk samples. Since so far we have only observed this effect in photon avalanche processes [9], we therefore attribute such spatial distribution of dots to the high non-linearity of the avalanche process. This effect may provide a direct means of observing the mode structure of light transmitted inside a fibre which has not yet been obtained previously.

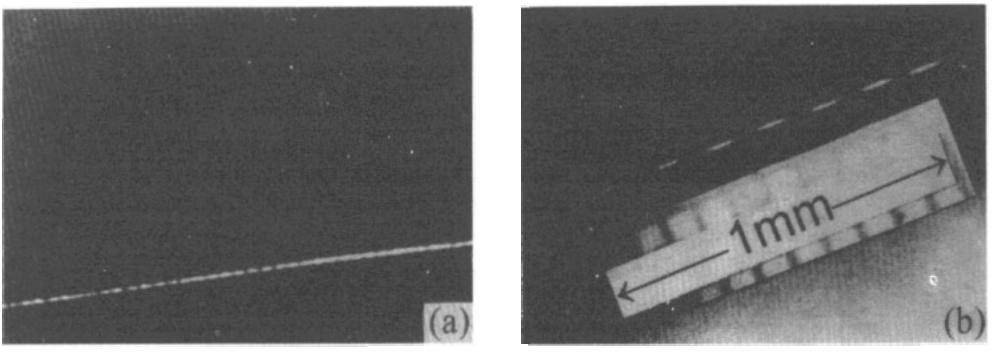

Figure 1. Pictures of the green dot structure along the fibre: (a) the distance between two neighbouring dots is about 1 mm; (b) observed with the microscope, there are about six even smaller dots in 1 mm.

Spectroscopic measurements and comparisons have been made for the distinct strong green emission in both bulk glass and fibre, as shown in figure 2. The well known transition $^4S_{3/2}$–$^4I_{15/2}$ of Er^{2+} is responsible for this emission. Measured from the fibre sides, the spectrum is the same as the spectrum from the bulk sample. However, the spectra measured from the fibre end are very different and they are fibre length dependent. In the long fibre, the fluorescence peak shifts from 550 to 556 nm. Two factors can contribute to this change: the Er^{3+} ion reabsorption for the resonant green emission and the emission transition $^2H_{9/2}$–$^4I_{13/2}$ (at about 556 nm). Also in the long fibre at a high pumping intensity, the amplified spontaneous emission (ASE) effect seems to take place at 556 nm (figure 2); this suggests that a large population in the $^2H_{9/2}$ level has been reached.

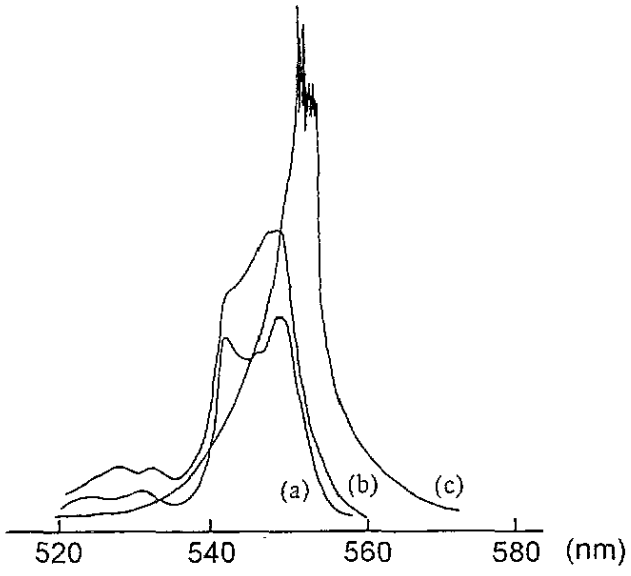

Figure 2. Spectra of green emission measured from a bulk sample (curve (a)), a short fibre (curve (b)) and a long fibre (curve (c)).

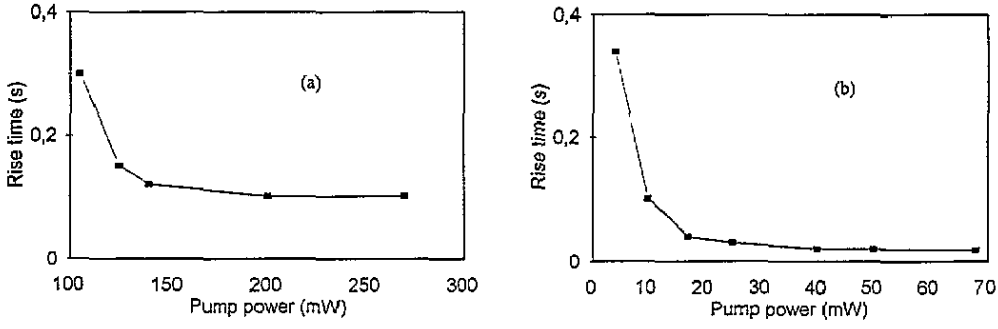

Figure 3. Dependences of rise time on the pump power in (a) a bulk sample and (b) a fibre.

The build-up process of this green avalanche emission is so slow that it is clearly observable by the naked eye. The rise time changes from 0.3 to 0.1 s in the bulk sample and from 0.3 to 0.02 s in the fibre in this measurement when pumping is varied by factors of 2.7 and 13, respectively (ratios of maximum to minimum pump powers in figures 3(a) and (b), respectively). The minimum rise time in the fibre is much smaller because of the much higher pump intensity achievable in the fibre, but it is still much larger than the lifetime of the $^4S_{3/2}$ level (less than 1 ms). Owing to the long build-up times for the avalanche emissions and induced absorption, some interesting phenomena can be observed; in the short fibre, the build-up process of the 550 nm emission as well as the emissions at all other wavelengths is in accordance with the build-up of induced avalanche absorption as measured through the transmitted pump power (figures 4(a) and (b)). However, in the long fibre, the 550 nm emission is composed of two processes: first a quick rise and then a decrease (see the top trace in figure 4(c)). This phenomenon is connected with both the build-up

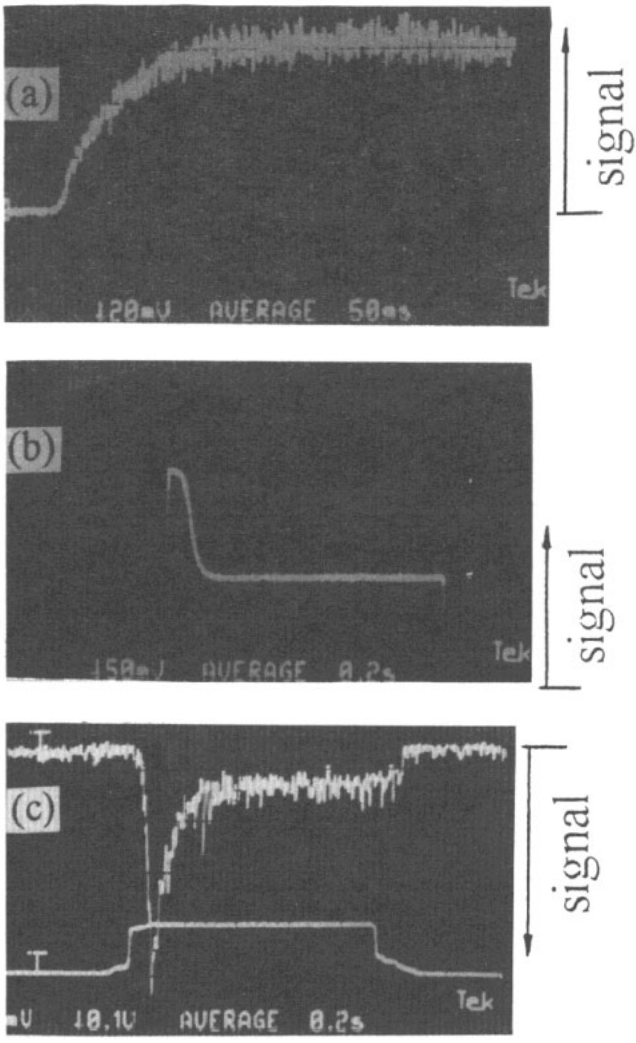

Figure 4. The oscilloscope traces of the build-up processes of (a) 550 nm fluorescence measured from the short fibre (8 cm), (b) transmitted pump power at 700 nm and (c) 550 nm fluorescence from the end of the longer fibre (90 cm).

process of induced absorption and the reabsorption of Er^{3+} ions at 550 nm, that is, just after switching on the pump power, the fibre is nearly transparent because the induced absorption has not yet been built up. So all parts of the fibre have about the same pump intensity; with gradually increasing induced absorption for the pump light, the avalanche emission became stronger and stronger. In the meantime, because of this induced absorption, the pump intensity along the fiber became weaker and weaker; so the avalanche build-up times for the different parts of the fibre are different. In the part near the input end, the pump intensity does not change obviously with time; the avalanche emission in this part simply experiences an increase until it reaches a stable state. However, the emission from this part which overlaps with the ground-state absorption is being reabsorbed owing to the high doping concentration and cannot reach the fibre end. In the meantime, in the end part of the fibre, the pump intensity decreases with time until it reaches a stable state (see figure 4(b)); so, in this part, the avalanche emission first increases quickly and then decreases on decrease in the pump intensity. The oscilloscope trace for the 550 nm emission from the fibre end

is then essentially the contribution of the emission from the end part. For those emissions which are not coincident with the ground-state absorption, such as $^4S_{3/2}$–$^4I_{13/2}$ (850 nm), $^4S_{3/2}$–$^4I_{11/2}$ (1220 nm) and $^2H_{9/2}$–$^4I_{13/2}$ (556 nm), they have the same time dependnece as the induced absorption because no reabsorption exists for these signals.

The multiphoon side-band absorption of Er^{3+} ions plays a key role in the beginning of the avalanche process. Before the pump reaches the avalanche threshold, we can still see some weak green luminescence which we attribute to the multiphonon anti-Stokes side band absorption to the $^4F_{9/2}$ level, and Stokes side-band absorption to $^4I_{9/2}$ followed by an excited-state absorption to high-lying states [12]. We have made a detailed study of the multiphonon side-band absorption in ZBLAN glass [13] from which we know that it varies linearly with the pump power. Here, the multiphoon energy gaps involved for exciting $^4F_{9/2}$ and $^4I_{9/2}$ are 1200 cm^{-1} and 1600 cm^{-1}, respectively; the corresponding absorption cross sections are estimated to be 1×10^{-27} cm^2 and 5×10^{-26} cm^2, respectively. It is much less than that for direct electronic absorption but here, with a high concentration, this absorption cannot be neglected.

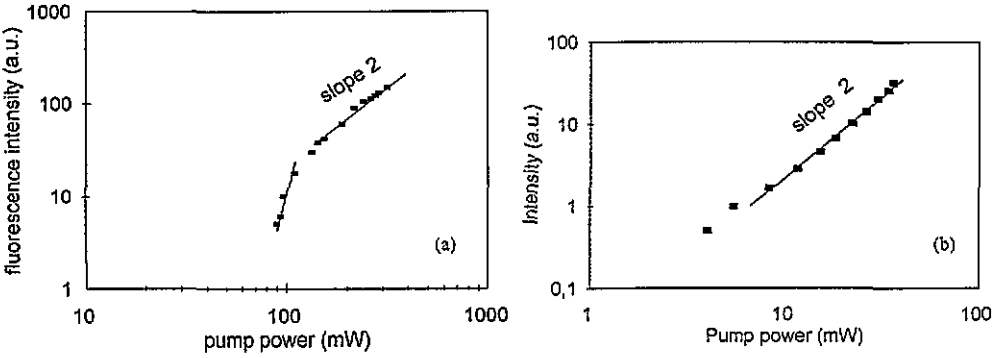

Figure 5. Fluorescence intensity of Er^{3+} ions versus incident pump power (a) in a bulk sample and (b) in a fibre (a.u., arbitrary units).

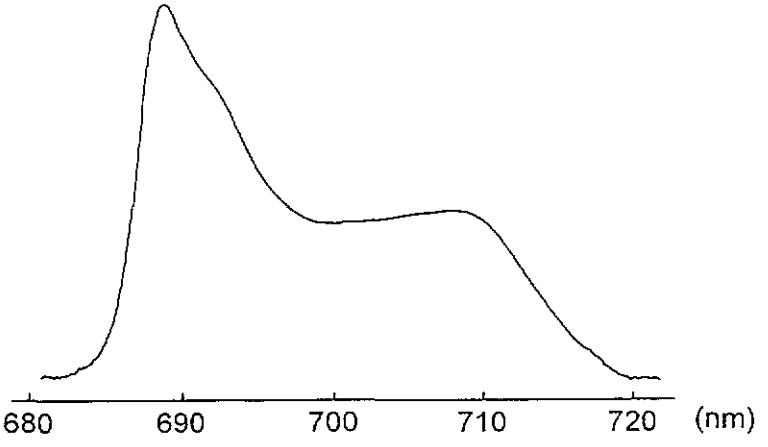

Figure 6. The excitation spectrum of the 550 nm avalanche up-converted fluorescence.

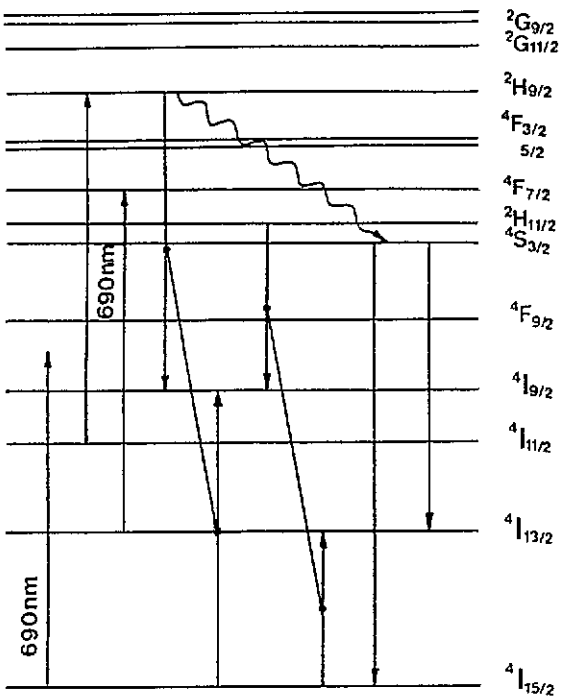

Figure 7. Energy levels of Er^{3+} ions and proposed mechanisms for the photon avalanche.

The dependences of the observed photon avalanche up-conversion on the pump power are shown in figure 5. The photon avalanche emissions appear when the incident pump powers reach about 100 mW and 4 mW, respectively, for the bulk and fibre samples; near the threshold, avalanche emissions experience a sharp rise (this is not very obvious in the fibre because of its relatively low threshold). In this stage, the population of the metastable level and therefore the excited-state absorption from this level increase vigorously by means of cross relaxation; thereafter, it keeps increasing with a slope of 2 in both cases. The excitation spectrum of the avalanche emission spans a range as wide as about 400 cm^{-1} (figure 6); this wide excitation spectrum suggests that more than one excited-state absorption participates in this process. According to the wavelength region of the excitation spectrum, three transitions are possibly involved: $^4I_{13/2}$–$^4F_{7/2}$, $^4I_{11/2}$–$^2H_{9/2}$ and $^4I_{9/2}$–$^2G_{11/2}$. However, as we have noted, in high-concentration samples the lifetimes of most excited states are obviously self-quenched except for the $^4I_{11/2}$ and $^4I_{13/2}$ levels; so we consider that this process is dominated by the first two transitions only. Also, when the photon avalanche has been built up under 690 nm excitation, some emissions at about 560 nm and 695 nm appear which correspond to the transitions $^2H_{9/2}$–$^4I_{13/2}$ and $^2H_{9/2}$–$^4I_{11/2}$, respectively. This indicates that the $^2H_{9/2}$ level has been populated in the photon avalanche process. All these facts help us to determine the mechanisms related to the 550 nm photon avalanche up-conversion. As shown in figure 7, the 700 nm laser excitation falls in between $^4F_{9/2}$ and $^4I_{9/2}$. A weak multiphonon side-band absorption exists which allows excitation of the Er ions to the $^4Fe_{9/2}$ and $^4I_{9/2}$ levels [9]; then excitation can reach $^4I_{11/2}$ and $^4I_{13/2}$ through non-radiative decay. The photon avalanche is then initiated by absorptions from $^4I_{11/2}$ to $^2H_{9/2}$ and from $^4I_{13/2}$ to $^4F_{7/2}$ which just coincide with the pump laser. When the pump incident power reached the critical threshold, the main cross relaxation process ($^2H_{9/2}$, $^4I_{15/2}$)–($^4I_{9/2}$, $^4I_{9/2}$) and $^2H_{11/2}$,

$^4I_{15/2}$)–($^4I_{9/2}$, $^4I_{13/2}$) followed by $^4I_{9/2}$–$^4I_{11/2}$ or $^4I_{11/2}$–$^4I_{13/2}$ non-radiative decay processes can sufficiently build up the populations of the $^4I_{11/2}$ or $^4I_{13/2}$ levels, respectively. Some other cross relaxations such as ($^4F_{7/2}$, $^4I_{15/2}$)–($^4I_{11/2}$, $^4I_{11/2}$), ($^4F_{3/2}$, $^4I_{15/2}$)–($^4I_{11/2}$, $^4I_{9/2}$) and ($^4F_{3/2}$, $^4I_{15/2}$)–($^4I_{9/2}$, $^4I_{11/2}$) are also possible. All these cross relaxations will populate the $^4I_{11/2}$ and $^4I_{13/2}$ levels, thereby participating to some extent in the photon avalanche.

In comparison with the avalanche process under 579 nm excitation [8], here we have two main cross relaxation processes, and the avalanche originates from two different levels $^4I_{11/2}$ and $^4I_{13/2}$ simultaneously. Also the excited-state absorption from $^4I_{11/2}$ to $^2H_{9/2}$ is larger than the absorption to $^2G_{9/2}$. These can explain the shorter rise time and lower threshold observed for 690 nm excitation.

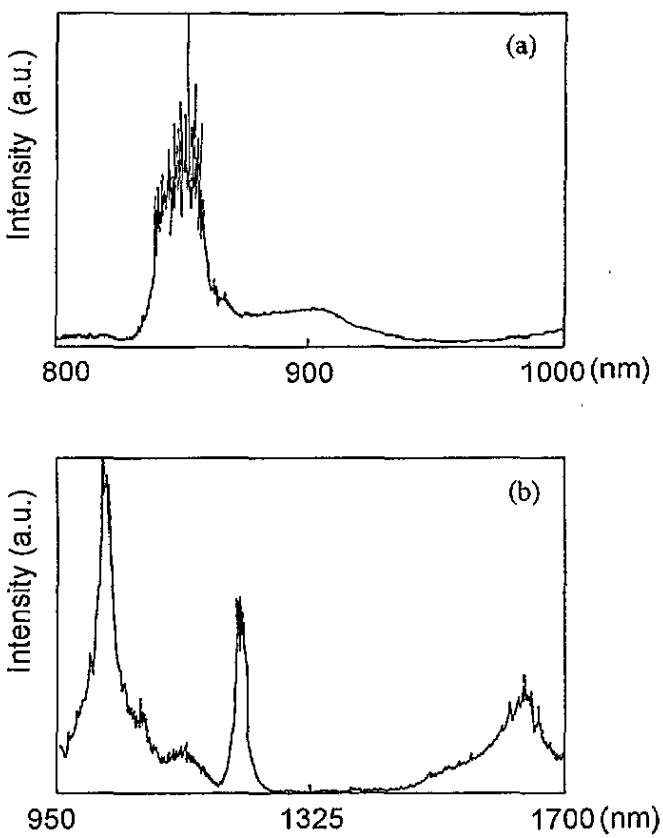

Figure 8. The IR spectra (800–1700 nm) measured from the end of the longer fibre (a.u., arbitrary units). In (a), ASE and laser oscillation takes place at 850 nm, even from the weak reflection of the fibre ends.

Besides avalanche emissions in the visible region, several strong IR emissions are observed in the avalanche-pumped fibre; these emissions are 850 nm ($^4S_{3/2}$–$^4I_{13/2}$), 1220 nm ($^4S_{3/2}$–$^4I_{11/2}$), 970 nm ($^4I_{11/2}$–$^4I_{15/2}$) and 1530 nm ($^4I_{13/2}$–$^4I_{15/2}$), as shown in figure 8; all these emissions are very strong. Emissions at 850 and 1220 nm have the same initial level ($^4S_{3/2}$) as that for the green emission; however, they have the advantage over the 550 nm emission that the final states of these two transitions ($^4I_{11/2}$ and $^4I_{13/2}$) can absorb the pump photon directly (to $^2H_{9/2}$ and $^4F_{7/2}$) and so contribute further to the avalanche process.

Because these two wavelengths are not reabsorbed, they could provide avalanche-pumped four-level laser transitions. The strong emissions at 970 and 1530 nm show that the $^4I_{11/2}$ and $^4I_{13/2}$ levels have been efficiently populated by the cross relaxation processes. So laser outputs at these wavelengths using the avalanche pumping could be achieved. In figure 8(a), some oscillations appear at 850 nm emission, this suggests to us that laser action takes place even from the weak reflection of the fibre ends.

Most of the photon avalanches found so far and reported in the literature are in systems with a lower phonon energy, and in most cases a low temperature is needed. We regard this as the influence of non-radiative decay on the metastable state. Materials with a low phonon energy will have a lower probability of non-radiative decay at a lower temperature and so metastable states are sufficiently long lived for an avalanche to take place. So we believe that, the higher the phonon energy, the higher the pump threshold of the photon avalanche; this could explain why we can obtain this effect in a ZBLAN glass, which is known for its lower phonon energy (580 cm^{-1} at cut-off frequency).

In summary, we have demonstrated another excitation path for a photon avalanche in an Er-doped ZBLAN fibre at room temperature. Mechanisms are proposed for modelling the dynamics in such system. This study could supply us with new pumping routes for laser operation and spectroscopy studies.

Acknowledgment

We would like to express our thanks to G Mazé from Le Verre Fluore for kindly supplying the Er-doped fluoride fibre.

References

[1] Chivian J S, Case W E and Eden D D 1979 *Appl. Phys. Lett.* **35** 124
[2] Case W E, Koch M E and Kueny A W 1990 *J. Lumin.* **45** 351
[3] Krasutsky N J 1983 *J. Appl. Phys.* **54** 1261
[4] Lenth W and Macfarlane R M 1990 *J. Lumin.* 45 346
[5] Oetliker U, Riley M J, May P S and Güdel H U, 1992 *J. Lumin.* **53** 553
[6] Pelletier-Allard N and Pelletier R 1987 *Phys. Rev.* B **26** 4425
[7] Ni H and Rand S C 1991 *Opt. Lett.* **16** 1424
[8] Auzel F, Chen Y H and Meichenin D 1994 *J. Lumin.* **60&61** 692
[9] Chen Y H and Auzel F 1995 *J. Phys. D: Appl. Phys.* **28** 207
[10] Koch M E, Kueny A W and Case W E 1990 *Appl. Phys. Lett.* **56** 1083
[11] Gomes A S L, Maciel G S, Araujo R E, Acioli L C and Araujo C B 1993 *Opt. Commun.* **103** 361
[12] Auzel F 1976 *Phys. Rev.* B **13** 2809
[13] Auzel F and Chen Y H 1994 *Opt. Quant. Electron.* **26** S559